Wei Tse Yang, FRCR
Jenny Chang, MRCP
Constantine Metreweli, FRCP, FRCR

Index terms:
Axilla, 997.8331, 07.33
Breast neoplasms, metastases, 997.8331, 07.33
Lymphatic system, neoplasms, 997.8331
Lymphatic system, US, 997.1298, 997.12983
Ultrasound (US), Doppler studies, 997.12983

Radiology 2000; 215:568–573

[1] From the Department of Diagnostic Radiology and Organ Imaging, Chinese University of Hong Kong, Prince of Wales Hospital, Shatin, NT, Hong Kong (W.T.Y., C.M.), and the Department of Medical Oncology, National University of Singapore, Singapore (J.C.). Received May 5, 1999; revision requested July 13; revision received August 9; accepted August 18. **Address correspondence to** W.T.Y.

© RSNA, 2000

Author contributions:
Guarantor of integrity of entire study, W.T.Y.; study concepts and design, W.T.Y.; definition of intellectual content, W.T.Y.; literature research, W.T.Y., J.C.; clinical studies, W.T.Y.; data acquisition, W.T.Y.; data analysis, W.T.Y., J.C.; statistical analysis, W.T.Y., J.C.; manuscript preparation, W.T.Y., J.C.; manuscript editing and review, J.C., C.M.

Patients with Breast Cancer: Differences in Color Doppler Flow and Gray-Scale US Features of Benign and Malignant Axillary Lymph Nodes[1]

PURPOSE: To document differences in color Doppler flow and gray-scale ultrasonographic (US) features between benign and malignant axillary lymph nodes in women with primary breast cancer.

MATERIALS AND METHODS: The longitudinal-transverse axis ratio and hilar status on color Doppler flow and gray-scale US images were prospectively studied for each of 145 axillary nodes in 135 women (74 palpable nodes in 69 women, 71 nonpalpable nodes in 66 women) with primary breast cancer. Intranodal flow distribution was described as peripheral, central, or central perhilar. Resistive and pulsatility indexes and peak systolic velocity were documented. For comparison of benign and malignant features, nodes were divided into three groups: palpable and nonpalpable, palpable, and nonpalpable.

RESULTS: Color flow was demonstrated equally well in benign and malignant axillary lymph nodes for all three groups. For all nodes, peripheral flow was significantly higher in malignant (118 of 153 nodes [77%]) than benign (45 of 160 nodes [28%]) nodes ($P < .001$); central flow and central perhilar flow were significantly greater ($P < .002$ and $< .001$, respectively) in benign than malignant nodes. Similar differences were not observed in nonpalpable nodes. The mean longitudinal-transverse axis ratio ($\pm$ SD) was significantly lower in malignant (1.8 ± 0.6) than benign (2.6 ± 0.8) nodes. Logistic regression analysis showed peripheral, central, and central perhilar flow and the mean longitudinal-transverse axis ratio to be significant independent predictors of malignancy.

CONCLUSION: Color Doppler flow and gray-scale US features applicable to the identification of disease in palpable axillary nodes in patients with breast cancer are not applicable to nonpalpable nodes.

Traditionally, axillary lymph node status has been an important prognostic factor in women with early-stage breast cancer (1–3) and is critical in the planning of systemic adjuvant therapy (4). However, axillary lymph node dissection is associated with substantial cost and morbidity, including seroma formation and arm edema. Increasingly, it is becoming recognized that not all patients need to undergo lymph node dissection, especially those without nodal metastases (5–7). Hence, the necessity for routine surgical axillary lymph node staging for all patients with breast cancer is increasingly controversial (6,7), and alternative accurate predictors of lymph node metastases would be important in selecting those patients who would benefit from axillary node dissection.

Clinical assessment and attempts at axillary staging by imaging with mammography, ultrasonography (US), and radionuclide techniques, including positron emission tomography, are currently inadequate (8–12). High-frequency US probes with improved spatial and

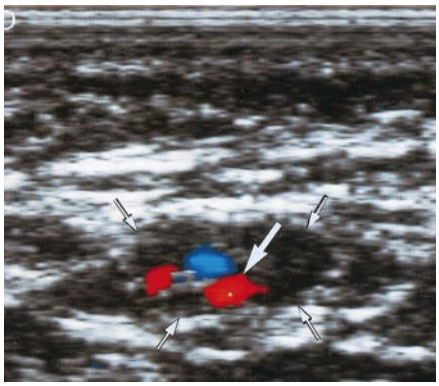

a.

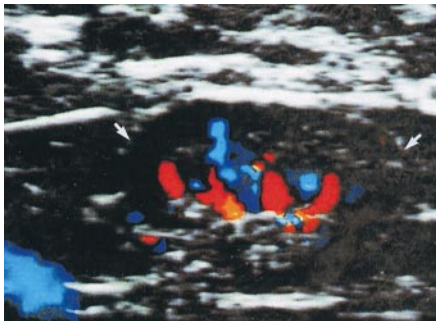

b.

Figure 1. Central perhilar vascularity on longitudinal color Doppler US images from two patients. **(a)** Simple hilar vessel (large arrow) within a normal axillary node (small arrows). **(b)** Central hilar centrifugal branches seen as blue and red linear structures within a normal axillary node (arrows).

contrast resolution have been used to study both primary breast cancer and superficial nodes, with encouraging results (13). US is valuable in the detection of enlarged nodes, while morphology is useful in the differentiation of benign from malignant disease (14). Furthermore, tumor vascularity, particularly in the breast, can be assessed in vivo with current techniques of color Doppler US (15,16). The morphologic and hemodynamic changes of tumor vessels have been used to differentiate benign from malignant tumors at duplex US (15).

Although a discriminatory role of color Doppler US has been shown for primary breast cancer (17), the value of Doppler spectral waveform analysis and color Doppler US in differentiating benign from malignant cervical lymph nodes remains controversial (18,19). To our knowledge, there is only one study in which color Doppler flow has been addressed as a diagnostic criterion for axillary nodal metastasis (20). However, no formal evaluation of the color Doppler US characteristics of axillary lymph nodes was performed in this earlier study.

The aim of our study was to determine prospectively the predictive value of gray-scale and color Doppler flow US features in axillary lymph nodes for the diagnosis of nodal metastases in patients with primary breast cancer.

MATERIALS AND METHODS

Study Population

One hundred forty-five lymph nodes in 135 women with breast cancer (mean age, 52 years; age range, 28–82 years) were prospectively studied with gray-scale and color Doppler US. Sixty-nine women had 74 palpable axillary lymph nodes, and 66 women had 71 nonpalpable axillary lymph nodes. In all palpable axillary nodes, notch-type, soft-tissue needle biopsy and/or fine-needle aspiration biopsy and cytologic analysis were performed prior to dissection. Nonpalpable nodes that were ultrasonographically abnormal according to previously published criteria (21) were also subjected to fine-needle aspiration biopsy and cytologic analysis. All patients subsequently underwent axillary dissection for histopathologic correlation. This study received local ethics committee approval, and informed consent was obtained from all patients.

Imaging and Color Doppler US

Conventional mammography and US of the breast were performed in all patients. Gray-scale and color Doppler flow US were performed after mammography with a 10-5-MHz linear-array transducer with a VST Master's Series unit (Diasonics, Santa Clara, Calif) or with an HDI 3000 unit (Advanced Technology Laboratories, Bothell, Wash).

Before histologic diagnosis, all women prospectively underwent US examination by one breast radiologist (W.T.Y.) who was blinded to the patient history. Gray-scale US evaluation of the breast and axilla was performed. The size of each lymph node was measured by using the longitudinal and transverse axis dimensions to obtain the longitudinal-transverse axis ratio. The presence of a normal central echogenic hilum was also documented.

Color Doppler flow US studies were performed with optimized color Doppler parameters set at low wall filter (50–100 Hz) and low velocity scale (pulse repetition frequency, 800–1500 Hz). Color gain was adjusted dynamically to maximize depiction of blood vessels while avoiding artifactual color noise. For each axillary lymph node, color Doppler interrogation was performed and the number and distribution of vessels were noted.

The vascular pattern of each node was then subjectively assessed according to modifications of the criteria by Na et al (22). Central perhilar vascularity was defined as a simple hilar vessel signal or centrifugal branches that were either central or eccentric (Fig 1); central nodal vascularity was defined as scattered spots or segments of vessel signals distributed within the node that were either radial, deformed radial, or aberrant multifocal (Fig 2); peripheral vascularity was defined as circumferential linear vascularity along the periphery of the node (Fig 3); and mixed vascularity was defined as more than one vascular pattern in a node. In lymph nodes where the hilum was absent, vascularity was described as either central, peripheral, or mixed.

Doppler spectral waveforms were obtained from three different vessels whenever possible for each node, and the highest value was selected. Spectral Doppler analysis was performed on the vessel with the most rigorous flow, and the peak systolic velocity, pulsatility index, and resistive index were noted. The probe was gently placed on the surface to avoid an artifactual increase in vascular resistance caused by compression of the superficial vessels. The sample volume of 1.5 mm was centered in the vessel, and the angle of insonation was kept at 60° or less in all examinations. The color Doppler features for all lymph nodes (combined) and for palpable and nonpalpable lymph nodes were then compared with the histologic diagnoses to determine their predictive value in differentiating benign from malignant disease.

Statistical Methods

Color flow and spectral Doppler, as well as gray-scale, parameters were analyzed by using the two-tailed χ^2 test with continuity correction, or the Fisher exact test, for the combined group (all lymph nodes), the palpable group, and the nonpalpable group. Multiple logistic regression analysis was performed to determine independent predictors of the significant individual variables obtained from univariate analysis.

RESULTS

Histopathologic Findings

A total of 145 axillary nodes were detected with US in 135 women with pri-

mary breast cancer. In the combined group, metastasis was confirmed with histologic findings in 66 (46%) of the 145 nodes. In the palpable group, metastasis was confirmed in 56 (76%) of the 74 nodes. In the nonpalpable group, nodal metastasis was present in 10 (14%) of the 71 nodes. All 10 nonpalpable metastatic nodes had fine-needle aspiration biopsy cytologic confirmation.

Color Doppler US Findings

Distribution of nodal vascularity.—The color Doppler characteristics of all lymph nodes are shown in Table 1. Color Doppler flow signal was present in more than 80% of malignant and benign axillary lymph nodes for all three groups.

For the combined group, there was greater peripheral flow in malignant nodes and greater central flow in benign nodes. The percentage of vessels with peripheral flow was significantly higher in malignant (77%) than in benign (28%) nodes ($P < .001$), while the percentages of central and central perhilar flow were significantly greater in benign (18% and 54%, respectively) than in malignant (5% and 18%, respectively) nodes ($P < .002$ and $P < .001$, respectively).

For the palpable group, a similar finding was observed. Flow was peripheral in 84% of malignant compared to 60% of benign nodes ($P = .009$), flow was central in 4% of malignant compared to 9% of benign nodes ($P = .142$), and flow was central perhilar in 13% of malignant compared to 31% of benign nodes ($P = .002$). However, no significant difference in flow distribution was shown between benign and malignant nonpalpable nodes. Comparison of vascular distribution between malignant and benign axillary nodes is graphically represented in Figure 4.

Doppler waveform of nodal vessel.—The resistive index, pulsatility index, and peak systolic velocities in this population overlapped between benign and malignant lymphadenopathy (Table 2), so that benign and malignant disease could not be distinguished on the basis of these indexes.

Gray-Scale Characteristics

Nodal shape and echogenic hilum.—Gray-scale characteristics of all lymph nodes are tabulated in Table 3. The longitudinal axis diameter of nodes ranged from 5 to 41 mm (mean, 19 mm), with no substantial difference in the mean diameter between benign (16 mm) and malignant (20 mm) lymph nodes. The mean longitudinal-transverse axis ratio (± SD) was significantly lower in malignant (1.8 ± 0.6) than in benign (2.6 ± 0.8) nodes ($P < .001$).

Using a longitudinal-transverse axis ratio of 2 or lower resulted in a sensitivity of 67% (44 of 66) and a specificity of 71% (56 of 79) in differentiating benign from malignant nodes. A sensitivity and specificity of 44% (29 of 66) and 92% (73 of 79), respectively, were obtained by using a longitudinal-transverse axis ratio of 1.5 or less.

Malignant nodes showed a significantly higher percentage of abnormal hila (55%) than did benign nodes (16%) ($P < .001$). At subset analysis, these significant differences were not observed in the palpable and nonpalpable groups.

Multiple Logistic Regression Analysis

Multiple logistic regression analysis of the pattern of vascularity gave a predictive accuracy of 79% for all lymph nodes and 75% for palpable nodes in determining nodal metastasis. The number of peripheral vessels was positively and the number of central vessels was negatively associated with malignancy. All color flow variables, including peripheral, central, and central perhilar flow and the mean longitudinal-transverse axis ratio, were significant independent predictors of malignancy (Table 4). The presence of an abnormal hilum was not independently associated with malignancy ($P = .465$).

DISCUSSION

US has consistently been shown to yield relatively high preoperative sensitivity in the prediction of axillary lymph node status (9,12,21). Findings of our prospective study showed significant differences in flow distribution and gray-scale features for benign and malignant nodes in patients with primary, operable breast cancer. Benign disease tended to retain central and/or central perhilar vascularity. The malignant group frequently showed peripheral and mixed vascularity in keeping with the characteristically tortuous and aberrant pattern of neovessels, which are displaced and encased by tumor. At multiple regression analysis, peripheral distribution of vascular flow and a low mean longitudinal-transverse axis ratio were independently associated with malignant disease, while central and central perhilar flow and a high mean longitudinal-transverse axis ratio were associated with benign nodal status.

Although the percentages of peripheral and central vessels were significantly different for benign and malignant axillary

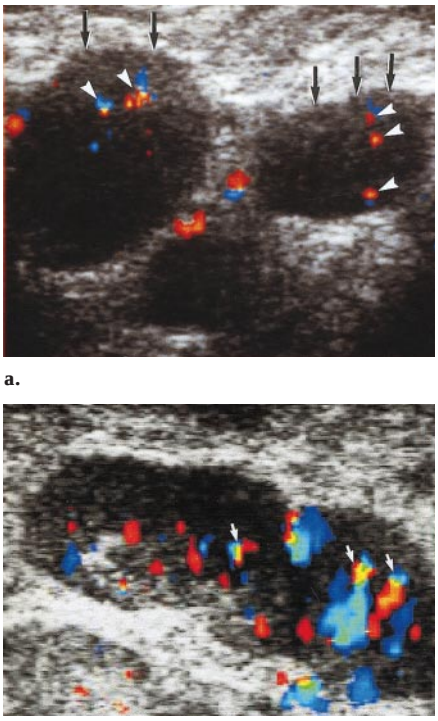

a.

b.

Figure 2. Central vascularity on **(a)** transverse and **(b)** longitudinal color Doppler US images from two patients. **(a)** Scattered spots of vessel signals (arrowheads) within rounded nodes with no central hila (arrows). **(b)** Vessel segments (arrows) radially aligned within a node with partially obliterated fatty hilum.

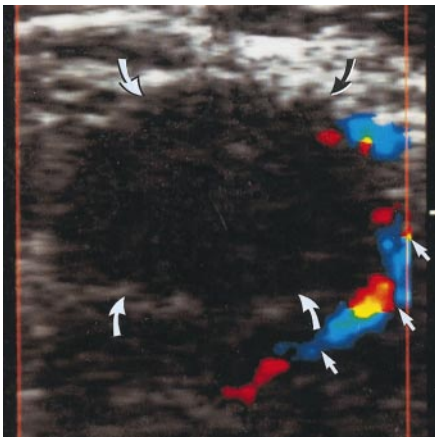

Figure 3. Peripheral vascularity on transverse color Doppler US image. Image shows linear vascularity (straight arrows) along the periphery of a node (curved arrows) with a low longitudinal-transverse axis ratio.

TABLE 1
Color Doppler US Features of 145 Lymph Nodes

Parameter	Combined Group			Palpable Group			Nonpalpable Group		
	Benign	Malignant	*P* Value	Benign	Malignant	*P* Value	Benign	Malignant	*P* Value
No. of patients	72	63	. . .	15	54	. . .	57	9	. . .
No. of lymph nodes									
Total	79	66	. . .	18	56	. . .	61	10	. . .
With vessels	68 (86)	56 (85)	>.05	17 (94)	47 (84)	>.05	51 (84)	9 (90)	>.05
No. of vessels									
Total	160	153	. . .	55	140	. . .	105	13	. . .
Arteries	106 (66)	103 (67)	>.05	34 (62)	95 (68)	>.05	70 (67)	8 (62)	>.05
Veins	54 (34)	50 (33)	>.05	21 (38)	45 (32)	>.05	35 (33)	5 (38)	>.05
Peripheral vessels	45 (28)	118 (77)	<.001	33 (60)	117 (84)	.009	12 (11)	1 (8)	.534
Central vessels	29 (18)	8 (5)	<.002	5 (9)	5 (4)	.142	24 (23)	3 (23)	.611
Central perhilar vessels	86 (54)	27 (18)	<.001	17 (31)	18 (13)	.002	69 (66)	9 (69)	.565
Mean no. of vessels ± 1 SD	2.4 ± 1.5	2.7 ± 2.3	>.05	3.2 ± 1.9	3.0 ± 2.4	>.05	2.1 ± 1.3	1.4 ± 0.5	>.05

Note.—Statistical univariate analysis of variables was conducted by using the χ^2 test with continuous correction. Numbers in parentheses are percentages.

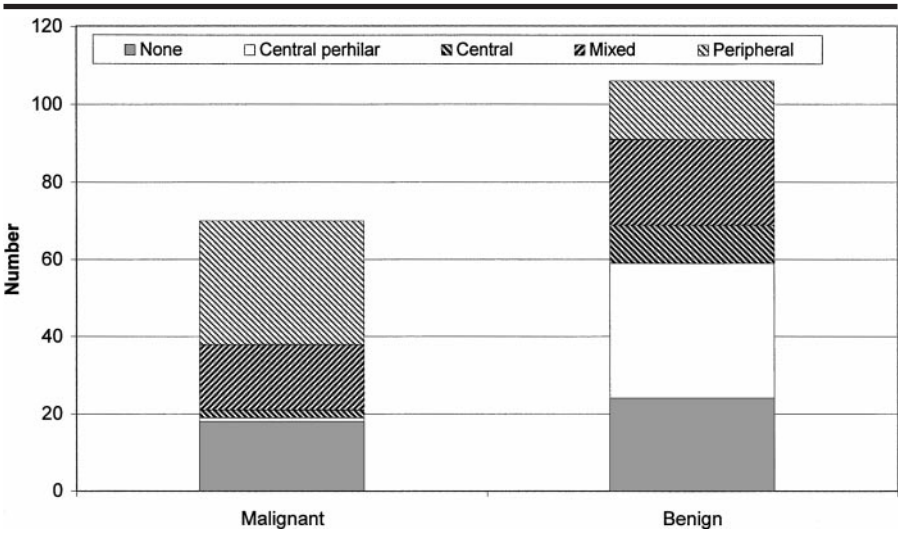

Figure 4. Graph of nodal vascular distribution in benign and malignant disease for the combined group. Flow is present in benign and malignant nodes. Malignant nodes show greater peripheral flow than benign nodes, while benign nodes show greater central flow than malignant nodes.

nodes, it should be emphasized that these numbers represent a significant difference between two proportions. A small difference between both groups can be detected if the sample size is large enough. These results could best be translated into clinical practice and management recommendations by suggesting that an axillary node with a low longitudinal-transverse axis ratio and predominantly peripheral flow is more likely to be malignant and that US-guided biopsy is warranted. Conversely, an axillary node with a high longitudinal-transverse axis ratio and predominantly central flow is more likely to be benign, and it may be reasonable to avoid biopsy.

In 1988, Morton et al (23) described flow signals in the hilum and center of reactive lymph nodes. Other reports (24,25) have shown the presence of flow in all enlarged lymph nodes, whether benign or malignant. It is believed that the hilar nodal artery, medullary arterioles, and sinuous capillaries in the cortex form the histologic basis for the longitudinal and radial configuration of normal nodal vascularity that appears on color Doppler US images (22). US-histopathologic correlation by Na et al (22) demonstrated residual subcapsular vessels in lymph tissue after central malignant lymph node infiltration. Another recent article (26) described intranodal angioarchitecture as a reliable aid in the differentiation between reactive and malignant superficial lymph nodes. Reactive lymph nodes tend to involve a diffuse histologic process and are more likely to preserve a normal vascularity pattern with central hilar vessels (26). Malignant changes caused by infiltrating tumor cells, on the other hand, lead to distortion and destruction of preexisting nodal vascular structures (26).

Malignant tumors a few millimeters in size generally stimulate neovascularization by means of the secretion of angiogenesis factors (27,28). These bizarre new blood vessels have thin walls without a muscular layer and frequently show chaotic anastomoses and shunts that end in amorphous spaces (29). Tumor vascularity has been detected with Doppler US in carcinoma of the breast, liver, and other organs (15,16,30,31). Although arteriovenous shunts and lack of muscular layers in vessels in malignant tumors have been reported (15,16), the same has not been reported in metastatic lymph nodes to date.

Color Doppler US provides information about flow and morphology. The use of high-frequency transducers increases the detectability of low-velocity signals from superficial structures. With the increased sensitivity in flow detection permitted with advancements in transducer and equipment technology, up to 85% of ultrasonographically normal axillary lymph nodes in women with no breast

TABLE 2
Spectral Doppler Features of 145 Lymph Nodes

Parameter	Combined Group			Palpable Group			Nonpalpable Group		
	Benign	Malignant	*P* Value	Benign	Malignant	*P* Value	Benign	Malignant	*P* Value
Mean resistive index ± 1 SD	0.67 ± 0.09	0.76 ± 0.12	>.05	0.69 ± 0.11	0.78 ± 0.12	>.05	0.66 ± 0.09	0.68 ± 0.10	>.05
Mean pulsatility index ± 1 SD	1.17 ± 0.52	1.29 ± 0.53	>.05	1.13 ± 0.42	1.30 ± 0.51	>.05	1.18 ± 0.56	1.24 ± 0.65	>.05
Mean peak systolic velocity ± 1 SD (cm/sec)	18.06 ± 8.41	24.1 ± 12.1	>.05	20.12 ± 10.10	24.61 ± 12.50	>.05	18.23 ± 7.94	21.45 ± 9.65	>.05

Note.—Statistical univariate analysis of variables was conducted by using the χ^2 test with continuous correction.

TABLE 3
Univariate Analysis of Variables of Gray-Scale US Features in 145 Lymph Nodes

Feature	Combined Group			Palpable Group			Nonpalpable Group		
	Benign	Malignant	*P* Value	Benign	Malignant	*P* Value	Benign	Malignant	*P* Value
No. of lymph nodes	79	66	. . .	18	56	. . .	61	10	. . .
Longitudinal-transverse axis ratio									
≤2	23 (29)	44 (67)	<.001	12 (67)	41 (73)	0.813	11 (18)	3 (30)	.699
≤1.5	6 (8)	29 (44)	<.001	5 (28)	27 (48)	0.212	2 (3)	2 (20)	.124
Abnormal hilum	13 (16)	36 (55)	<.001	11 (61)	35 (62)	<1.000	2 (3)	1 (10)	.370
Mean longitudinal-transverse axis ratio ± 1 SD	2.6 ± 0.8	1.8 ± 0.6	<.001	2.1 ± 0.9	1.7 ± 0.6	.073	2.7 ± 0.7	2.3 ± 0.8	.117

Note.—Numbers in parentheses are percentages.

disease show the presence of color Doppler flow (32). It is thus inappropriate to diagnose axillary lymph node metastasis on the basis of the presence of color Doppler flow signal alone. The results of our study lend further support to this premise, as 86% of benign and 85% of malignant nodes showed the presence of color flow.

The results of pulsed Doppler US (resistive index, pulsatility index, and peak systolic velocity) in this study are in contradiction with those of previous studies (18,19,22,33), which were primarily studies on cervical lymph nodes. Findings of these studies showed a higher resistive index and pulsatility index in malignant nodes than in benign nodes (18,19,22,33). No significant difference was demonstrated in the resistive index and pulsatility index between malignant and benign axillary disease in our study, which thus precludes the use of pulsed Doppler US in obviating axillary nodal biopsy.

A sensitivity and specificity of 67% and 71%, respectively, were obtained by using a longitudinal-transverse axis ratio of 2 or less to differentiate benign from malignant nodes in this study. The presence of an abnormal hilum, although seen in a significantly higher percentage of malignant than benign nodes, was not a significant independent predictor of malignancy. These findings are at variance with a recent axillary lymph node in vitro report that described the absence of hilum as the sign with the highest positive predictive value in nodes 10 mm or larger (34). Nodal size beyond 1–1.5 cm has been employed as the sole criterion to assess malignancy at computed tomography and magnetic resonance imaging, but this has been not been shown to be helpful at US (13).

TABLE 4
Multiple Logistic Regression Analysis of Variables in 145 Lymph Nodes

Variable	Coefficient	SE	*P* Value
Central perhilar vessel	−0.8035	0.2712	.003
Central vessel	−0.9240	0.4564	.049
Peripheral vessel	+0.2776	0.1450	.056
Longitudinal-transverse axis ratio	−1.2643	0.3682	<.001

The contribution of color Doppler and gray-scale US to identifying diseased axillary lymph nodes in women with primary breast cancer is especially pertinent given the current interest in seeking methods other than axillary dissection or sampling, notably sentinel node imaging and surgery, for staging and treating breast cancer. These promising findings may have clinical applicability if imaging and flow features can be used to identify nodes that merit imaging-guided biopsy. This method may be useful in the diagnosis and management of breast cancer, particularly early invasive and in situ cancers, for which axillary nodal dissection is not routinely practiced, in an effort to reduce morbidity from surgery. An easy and reproducible method of diagnosis and follow-up of axillary nodal disease is desirable with the current shift toward neoadjuvant medical and hormonal therapy for primary breast cancer.

An important caveat to this study is that the differences in the proportions of peripheral, central, and central perhilar vessels between benign and malignant palpable axillary nodes were not demonstrated in the nonpalpable group; thus, caution should be employed when applying such criteria to the latter. Features applicable to the identification of malignant involvement of palpable nodes are not applicable to nonpalpable nodes. Identification of metastatic involvement of nonpalpable nodes by using noninvasive techniques unfortunately remains an unfulfilled goal. Larger studies are required in patients with nonpalpable lymph node disease to determine its role in this subgroup of women.

References

1. Wilking N, Rutqvist LE, Cartensen J, Mattson A, Skoog L, participating members of the Stockholm Breast Cancer Study Group. Prognostic significance of axillary nodal status in primary breast cancer in relation to the number of resected nodes. Acta Oncol 1992; 31:29–35.
2. Bryan RM, Mercer RJ, Bennett RC, Rennie GC. Prognostic factors in breast cancer and the development of a prognostic index. Br J Surg 1986; 73:267–271.
3. Haybittle JL, Blamey RW, Elston CW, et al. A prognostic index in primary breast cancer. Br J Cancer 1982; 45:361–366.
4. Early Breast Cancer Triallists' Collaborative Group (EBCTCG). Systemic treatment of early breast cancer by hormonal, cytotoxic, or immune therapy: 133 randomized trials involving 31,000 recurrences and 24,000 deaths among 75,000 women. Lancet 1992; 339:1–15.
5. Recht A, Houlihan MJ. Axillary lymph nodes and breast cancer: a review. Cancer 1995; 76:1491–1512.
6. Cady B. The need to reexamine axillary lymph node dissection in invasive breast cancer (editorial). Cancer 1994; 73:505–508.
7. Ruffin WK, Stacey-Clear A, Younger J, Hoover HC. Rationale for routine axillary dissection in carcinoma of the breast. J Am Coll Surg 1995; 180:245–251.
8. McLean RG, Ege GN. Prognostic value of axillary lymphoscintigraphy in breast carcinoma patients. J Nucl Med 1986; 27: 1116–1124.
9. Pamilo M, Soiva M, Lavast EM. Real-time ultrasound, axillary mammography, and clinical examination in the detection of axillary lymph node metastases in breast cancer patients. J Ultrasound Med 1989; 8:115–120.
10. Tjandra JJ, Sacks NPM, Thompson CH, et al. The detection of axillary lymph node metastases from breast cancer by radiolabelled monoclonal antibodies: a prospective study. Br J Cancer 1989; 59:296–302.
11. Adler LP, Crowe JP, Alkaisi NK, Sunshine JL. Evaluation of breast masses and axillary lymph nodes with [F-18]2-deoxy-2-fluoro-D-glucose PET. Radiology 1993; 187: 743–750.
12. Lam WWM, Yang WT, Chan YL, Stewart IET, Metreweli C, King W. Detection of axillary lymph node metastases in breast carcinoma by technetium-99m-sestamibi breast scintigraphy, ultrasound and conventional mammography. Eur J Nucl Med 1996; 23:498–503.
13. Vassallo P, Wernecke K, Roos N, Peters PE. Differentiation of benign from malignant superficial lymphadenopathy: the role of high resolution US. Radiology 1992; 183: 215–220.
14. Vassallo P, Edel G, Roos N, Naguib A, Peters PE. In-vitro high-resolution ultrasonography of benign and malignant lymph nodes: a sonographic-histopathologic correlation. Invest Radiol 1993; 28:698–705.
15. Schoenberger SG. Breast neoplasms: duplex sonographic imaging as an adjunct to diagnosis. Radiology 1988; 168:665–668.
16. Cosgrove DO, Bamber JC, Davey JB, Mckinna JA, Sinnett HD. Color Doppler signals from breast tumors. Radiology 1990; 176:175–180.
17. Cosgrove DO, Kedar RP, Bamber JC, et al. Breast diseases: color Doppler US in differential diagnosis. Radiology 1993; 189:99–104.
18. Chang DB, Yuan A, Yu CJ, Luh KT, Kuo SH, Yang PC. Differentiation of benign and malignant cervical lymph nodes with color Doppler sonography. AJR Am J Roentgenol 1994; 162:965–968.
19. Choi MY, Lee JW, Jang KJ. Distinction between benign and malignant causes of cervical, axillary and inguinal lymphadenopathy: value of Doppler spectral waveform analysis. AJR Am J Roentgenol 1995; 165:981–984.
20. Walsh J, Dixon JM, Chetty U, Paterson D. Colour Doppler studies of axillary node metastases in breast carcinoma. Clin Radiol 1994; 49:189–191.
21. Yang WT, Ahuja AT, Tang A, Suen M, King W, Metreweli C. High frequency ultrasound detection of axillary lymph node metastases in breast cancer. J Ultrasound Med 1996; 15:241–246.
22. Na DG, Lim HK, Byun HS, Kim HD, Ko YH, Baek JH. Differential diagnosis of cervical lymphadenopathy: usefulness of color Doppler sonography. AJR Am J Roentgenol 1997; 168:1311–1316.
23. Morton MJ, Charboneau JW, Banks PM. Inguinal lymphadenopathy simulating a false aneurysm in color flow Doppler sonography. AJR Am J Roentgenol 1988; 151: 115–116.
24. Swischuk LE, Desai PB, John SD. Exuberant blood flow in enlarged lymph nodes: findings on color flow Doppler. Pediatr Radiol 1992; 22:419–421.
25. Mountford RA, Atkinson P. Doppler ultrasound examination of pathologically enlarged lymph nodes. Br J Radiol 1979; 52:464–467.
26. Tschammler A, Ott G, Schang T, Seelbach-Goebel B, Schwager K, Hahn D. Lymphadenopathy: differentiation of benign from malignant disease—color Doppler US assessment of intranodal angioarchitecture. Radiology 1998; 208:117–123.
27. Folkman J, Merler E, Abernathy C, Williams G. Isolation of a tumor factor responsible for angiogenesis. J Exp Med 1971; 33:275–278.
28. Schor AM, Schor SL. Tumour angiogenesis. J Pathol 1983; 141:385–413.
29. Strickland B. The value of arteriography in the diagnosis of bone tumors. Br J Radiol 1959; 32:705–713.
30. Ramos IM, Taylor KJW, Kier R, Burns PN, Snower DP, Carter D. Tumor vascular signals in renal masses: detection with Doppler US. Radiology 1988; 168:633–637.
31. Shimamoto K, Sakuma S, Ishigaki T, Ishigachi T, Itoh S, Fukatsu H. Hepatocellular carcinoma: evaluation with color Doppler US and MR imaging. Radiology 1992; 182:149–153.
32. Yang WT, Metreweli C. Color Doppler flow in normal axillary lymph nodes. Br J Radiol 1998; 71:381–383.
33. Wu CH, Chang YL, Hsu WC, Ko JY, Sheen TS, Hsieh FJ. Usefulness of Doppler spectral analysis and power Doppler sonography in the differentiation of cervical lymphadenopathies. AJR Am J Roentgenol 1998; 171:503–509.
34. Feu J, Tresserra F, Fabregas R, et al. Metastatic breast carcinoma in axillary lymph nodes: in vitro US detection. Radiology 1997; 205:831–835.